sciendo | Journal of Electrical Bioimpedance | JoEB bioimpedance.net

J Electr Bioimp, vol. 11, pp. 62-71, 2020
Received 28 May 2020 / published 25 Jul 2020
https://doi.org/10.2478/joeb-2020-0010

In silico and *in vitro* conductivity models of the left heart ventricle

Leonie Korn[1,4], Simon Lyra[1], Daniel Rüschen[1], Dmitry Telyshev[2,3], Steffen Leonhardt[1], Marian Walter[1]

1. *Medical Information Technology, RWTH Aachen University, Aachen, Germany*
2. *Institute for Biomedical Systems, National Research University of Electronic Technology, Moscow, Russian Federation*
3. *Institute for Bionic Technologies and Engineering, I. M. Sechenov First MSMU, Moscow, Russian Federation*
4. *E-mail any correspondence to: korn@hia.rwth-aachen.de*

Abstract

Ventricular Assist Devices (VADs) are used to treat patients with cardiogenic shock. As the heart is unable to supply the organs with sufficient oxygenated blood and nutrients, a VAD maintains the circulation to keep the patient alive. The observation of the patient's hemodynamics is crucial for an individual treatment; therefore, sensors to measure quantifiable hemodynmaic parameters are desirable.

In addition to pressure measurement, the volume of the left ventricle and the progress of muscle recovery seem to be promising parameters. Ongoing research aims to estimate ventricular volume and changes in electrical properties of cardiac muscle tissue by applying bioimpedance measurement. In the case where ventricular insufficiency is treated by a catheter-based VAD, this very catheter could be used to conduct bioimpedance measurement inside the assisted heart. However, the simultaneous measurement of bioimpedance and VAD support has not yet been realized, although this would allow the determination of various loading conditions of the ventricle. For this purpose, it is necessary to develop models to validate and quantify bioimpedance measurement during VAD support.

In this study, we present an *in silico* and an *in vitro* conductivity model of a left ventricle to study the application of bioimpedance measurement in the context of VAD therapy. The *in vitro* model is developed from casting two anatomical silicone phantoms: One phantom of pure silicone, and one phantom enriched with carbon, to obtain a conductive behavior close to the properties of heart muscle tissue. Additionally, a measurement device to record the impedance inside the ventricle is presented. Equivalent to the *in vitro* model, the *in silico* model was designed. This finite element model offers changes in material properties for myocardium and the blood cavity.

The measurements in the *in vitro* models show a strong correlation with the results of the simulation of the *in silico* model. The measurements and the simulation demonstrate a decrease in impedance, when conductive muscle properties are applied and higher impedances correspond to smaller ventricle cross sections.

The *in silico* and *in vitro* models are used to further investigate the application of bioimpedance measurement inside the left heart ventricle during VAD support. We are confident that the models presented will allow for future evaluation of hemodynamic monitoring during VAD therapy at an early stage of research and development.

Keywords: VAD, electrical properties heart, heart volumetry, silicone conductivity, FEM heart

Introduction

Cardiogenic shock (CS) is still a leading cause of death in developed countries [1]. In the case of a CS, adequate blood circulation is not maintained due to a reduced pump performance in the damaged left ventricle. If untreated, the lack of oxygen and nutrients in the periphery can lead to death. The VAD systems, in particular minimal-invasive rotary blood pumps, are used for the treatment of CS to perpetuate blood circulation and save the patient's life.

The state of the art in VAD therapy is to operate the impeller at a constant rotational speed at the discretion of the attending physician. However, individual hemodynamic monitoring to observe the pressures and volumetric flows in the circulation are needed to know the patient's actual demand for an optimal therapy [2], [3]. Therefore, parameters in VAD therapy must be derived to qualify the heart condition and the needs of the patient. To date, the integration of pressure sensors on the surface of a VAD has been completed successfully [4], whereas an accurate measure to monitor the preload of the heart is

missing. Life-threatening adverse events, such as suction, resulting in a shrinkage of left ventricular volume (LVV) are frequently observed complications. A low LVV can lead to a shift of the septum and affects the electrical activation of the heart. By contrast, if the LVV is too high, pulmonary edema due to the high preload may be caused. Therefore, the monitoring of LVV is essential to account for the observation of various loading conditions, which can currently only be determined for one point in time using imaging modalities.

We believe that using bioimpedance measurements during VAD treatment will provide additional information about the condition of the heart; however, the interaction between bioimpedance measurement and VAD support has not yet been properly assessed. The placement of more than four electrodes on the surface of a catheter-based VAD is similar to the setup proposed by Baan et al. [5]. A current is injected into the outer electrodes, spanning the electric field, whereas the inner electrodes are used to measure voltages depending on the surrounding tissue. The admittance calculated correlates to the volume of the left ventricular blood cavity. Due to non-linear effects of the electrical field spread by two point charges, Wei et al. [6] proposed a new algorithm for volume computation of the blood cavity. Nevertheless, this method still requires calibration, for instance with ultrasound. Furthermore, the method neglects material boundaries, which have a huge impact on the electric field distribution. Additionally, it has been shown that the electrical properties of myocardial tissue change during ischemia [7]. We speculate that this information can be used to derive an estimate for the condition of myocardial tissue during CS. All this leads to the consideration of applying bioimpedance measurements for the improvement of VAD treatment.

In this work, we present the validation of an *in silico* and two *in vitro* models of the left heart ventricle intended to be used for the application of bioimpedance measurement during VAD support. In the future, these models will be used to observe changes in blood volume and properties of heart muscle tissue using bioimpedance measurement during VAD support both theoretically and practically, while simultaneously providing rapid testing, reproducibility, cost efficiency and the avoidance of animal testing.

The *in silico* model is built as a finite element model (FEM) to perform detailed studies of the electric field and current pathways in the heart. The electrical material properties can be modified for each finite element. Further, this model will be used to find optimal electrode placement on the VAD to monitor ventricular volume and dynamic changes of tissue properties.

The *in vitro* model of the left ventricle consists of two phantoms made from silicone. One phantom was cast from pure silicone; the second is customizable with carbon to adjust its electrical properties to values similar to that of heart muscle tissue. Both models combine different advantages so that they are highly suitable for the investigation of bioimpedance measurement and the integration of VADs and thus may contribute to an improvement of therapy.

Additionally, we present, as a first prototype, a miniaturized and cost-effective hardware setup. The latter is designed to compare the *in vitro* with the *in silico* model while measuring the impedance continuously over time using a 10-electrode catheter that emulates the placement of electrodes on the VAD and in the ventricle.

In vitro model and measurement system

Customized silicone

An elastic material with conductive electrical properties is required in order to build a realistic model of a human heart. In this section, the method to customize the electrical properties of silicone for the *in vitro* model is described. We selected silicone, because the elastic properties of this material are similar to those of heart muscle, it is more durable, than for example, agar-agar, and easy to process. The most important advantage is that various additives can be combined with silicone to mimic the electrical properties of heart muscle tissue.

We selected silicone with a shore scale of A00 (Silikonfabrik.de, Ahrensburg, Germany), which is in the range of the elastic properties of heart tissue, for the *in vitro* ventricle phantom. Depending on the point of time in the cardiac cycle, heart muscle tissue has an elasticity modulus between $20\,\mathrm{kPa}$ and $280\,\mathrm{kPa}$ [8]. Silicone with a shore scale of A00 has an elasticity modulus of about $100\,\mathrm{kPA}$ according to Gent et al. [9]. The electrical conductivity of pure silicone is about $\sigma_s = 10^{-10}\,\frac{\mathrm{S}}{\mathrm{m}}$. Carbon black powder (VULCANR XC72, Cabot Corporation, Boston, USA) together with carbon cutlets with an average length of $3\,\mathrm{mm}$ (R&G Faserverbundwerkstoffe GmbH, Waldenbuch, Germany) were mixed into the silicone to manipulate the electrical properties. A concentration variation to reach the percolation limit (the threshold above a strong increase in conductivity can be measured) was conducted. Therefore, a mixture of both materials, carbon powder and carbon cutlets, was added to the silicone by simultaneously guaranteed proper compounding. Different samples with a concentration of $1\,\%$ of carbon black powder and a variation of carbon cutlet concentration (between $0.7\,\%$ and $1\,\%$) were investigated. All samples were cast into a standardized cylindrical form with a diameter of $28\,\mathrm{mm}$, and subsequently degassed ($100\,\mathrm{kPa}$) and cured to ensure reproducibility. A weight of $35.6\,\mathrm{g}$ was placed on all samples to ensure the same contact pressure, since the contact area influences the impedance measured. An LCR-meter E4980A from Keysight (Santa Rosa, USA) was applied

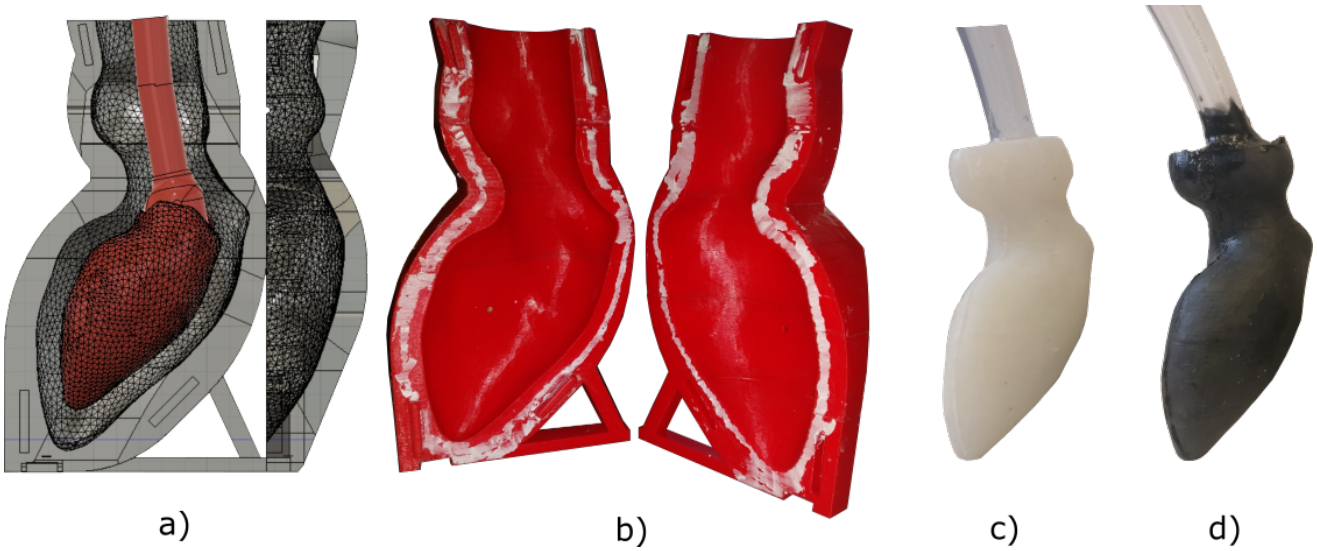

Fig. 1: a) CAD model with the inner wax-/ polyvinylalcohol-core; b) 3D-printed casting molds from polylactide; c) Resulting insulating ventricle from silicone; d) Resulting conductive ventricle from silicone and carbon.

for the analysis of samples. All measurement results are described in detail in [10]. To summarize the results from our previous work: all samples had pure ohmic behavior. Difficulties in homogenization of samples were experienced when using only carbon cutlets. Instead, a mixture of both carbon cutlets and powder showed homogeneous samples and reproducible results. A conductivity of about $\sigma_C = 0.306\,\frac{\mathrm{S}}{\mathrm{m}}$ within the range of physiological heart tissue $(0.05\,\frac{\mathrm{S}}{\mathrm{m}} - 0.3\,\frac{\mathrm{S}}{\mathrm{m}})$ was reached with a concentration of $1\,\%$ of carbon black powder and $0.7\,\%$ of carbon cutlets.

Ventricle phantom

Three dimensional (3D)-printed low-cost molds that replicate the anatomical shape of a left ventricle were developed to cast the *in vitro* silicone phantoms. Therefore, data from embodi3D [11] of a left ventricle was taken from a computer tomographic image series consisting of 300 slices with a slice thickness of $0.4\,\mathrm{mm}$ each. The model was simplified by removing the left atrium, pulmonary veins and the coronary arteries. Additionally, the ventricle walls were smoothed. These simplifications allowed for 3D printing of molds and the replication of the inner blood cavity. The modification of the ventricle was done with Fusion 360 (AUTODESK Corporation, San Rafael, USA), a computer-aided design (CAD) software. The simplified ventricle shape was used to construct the 3D casting molds by cutting the volume of the ventricle out of a cuboid. The volume of the cuboid was reduced to a minimum without affecting the stability of the casting molds to save printing material and time. The casting molds were printed with polylactide using a wall thickness of $1.75\,\mathrm{mm}$ and a layer thickness of $0.2\,\mathrm{mm}$. The CAD model and the 3D-printed casting molds are shown in Fig. 1a) and 1b), respectively.

The manufacturing of hollow ventricle phantoms was necessary to emulate the inner blood cavity. Therefore, we tested two methods to obtain a soluble core. Paraffin wax was poured into a negative core mold and then boiled out of the silicone phantom. This method required additional molds but was highly cost-effective. As an alternative, 3D-printed polyvinylalcohol cores were used and separated from the silicone by dissolving in warm water. Here, the reproducibility of the phantom became easier, as fine structures can be reproduced consistently. Furthermore, the 3D-printing of the blood cavity allows for a rapid customization of the model. The development of the core (red core in Fig. 1a)) in CAD was done by scaling the ventricle used for the casting molds to an end-diastolic volume of about $120\,\mathrm{ml}$. This operating point is typical for measurement of PV-Loop related parameters (e.g. end diastolic volume). Smaller ventricle sizes can be simulated by applying external pressure or internal suction displacing the walls according to the volume shift. In addition, the aorta was replaced by a cylindrical shape such that a hose can be poured directly into the silicone phantom.

Two ventricle phantoms were cast for comparison. One made of pure silicone (see Fig. 1c)) and the other made of silicone with a carbon concentration (see Fig. 1d)) as described in the previous section *Customized silicone*. A wall thickness of $8\,\mathrm{mm} - 10\,\mathrm{mm}$ was fabricated with a blood volume of about $140\,\mathrm{ml}$, including the cylindrical part of the aorta, which is within the physiological range of a man's heart having a wall thickness between $4\,\mathrm{mm} - 10\,\mathrm{mm}$ and a diastolic volume of $67\,\mathrm{ml} - 155\,\mathrm{ml}$ [12]. Both ventricles were connected to a water tank with a polyvinylchlorid (PVC) hose.

A saline solution with a conductivity of $\sigma_{\text{saline}} = 0.658\,\frac{\text{S}}{\text{m}}$ close to the conductivity of blood $\sigma_{\text{blood}} = 0.701\,\frac{\text{S}}{\text{m}}$ was used to fill the hollow ventricles. The conductivity of the solution was validated with the conductivity meter HI 8733 (HANNA Instruments, Woonsocket, Rhode Island, USA).

Impedance measurement system

The impedance measurement system for continuous monitoring inside the *in vitro* model is based on the arrangement defined by Baan et al. [5]. Ten electrodes are attached to a catheter to replicate a beneficial electrode configuration for catheter-based VADs. This allows for the future application of our device in animal experiments as well. A miniaturized and low-cost measurement system was developed, which records the impedance in real-time while simultaneously allowing for changes of measurement parameters, such as measurement frequency, sampling rate and signal pre-amplification. The impedance measurements were performed using a 6−French ten-electrode electrophysiology catheter (VANGUARD AG, Berlin, Germany). The electrodes are made from platinum and evenly distributed on the catheter at a distance of 5 mm.

We created a modular hardware configuration to allow for rapid modifications in the prototype phase. The schematic arrangement of the printed circuit boards (PCBs) designed is shown in Fig. 2. It consists of a controller area network (CAN) communication board, the Launchpad MSP430G2553 (Texas Instruments Incorporated, Dallas, USA), a power supply PCB and a measurement PCB.

The power supply PCB provides 3.3 V and 5 V by two low-dropout regulators. Additionally, a charge pump is integrated which generates −3.3 V for multiplexer and amplifier circuit.

The centerpiece of the measuring unit is the microcontroller MSP430G2553 integrated on the launchpad, which is used for communication via serial peripheral interface with the integrated circuits on the CAN-PCB and the measurement PCB.

The analog front-end AFE4300 from Texas Instruments Incorporated (Dallas, USA), which is a cost-effective and highly integrated circuit used in body fat scales, featuring bioelectrical impedance analysis, is mounted on the measurement PCB. The bioelectrical impedance analysis function can be used to perform reliable four-point impedance measurements between 1 kHz and 100 kHz obtaining magnitude and phase for various frequencies. It should be noted that an impedance range of $1\,\Omega - 2.8\,\text{k}\Omega$ is covered by using the AFE4300 front-end for body fat scales. In our measurement setup, the expected impedance range is approximately between $0\,\Omega$ and $100\,\Omega$, resulting in low utilization of the 16 Bit resolution range of the analog-to-digital converter (ADC), which is embedded in the AFE4300. However, this problem was solved by an optional pre-amplification of the voltage signal integrated onto the measurement PCB. Additionally, the PCB includes the multiplexer DG4051EEG-T1-GE3 (Vishay Intertechnology, Inc., USA, Malvern) to switch between different sensing electrodes of the catheter. The current injection is permanently attached to the outer electrodes (1 and 10) of the electrophysiology catheter. The ADC of the AFE4300 can convert the voltage difference of two electrodes simultaneously. We applied external multiplexing to enable faster sensing at all electrodes $(2-9)$, since the internal multiplexing of the AFE4300 is too slow to perform heart cycle synchronous measurements. The maximal conversion rate for one measurement is 95 Hz, which results from the maximal sampling rate of the ADC, the time for multiplexing of all channels and communication delays. A conversion rate of 4 Hz was selected for this study. The AFE4300 is calibrated with known resistors to convert the values recorded by the ADC into impedance values. While the calibration with two reference values can be described by a straight-line, the use of four resistors requires a linear multi-point interpolation, so that the four values measured are used to calculate three straight-line equations. Therefore, a calibration network consisting of four resistances is integrated on the measurement PCB. The calibration resistances selected for this study can be taken from Table 1. The AFE4300 has two different operation modes for further processing of the measurement signal. Both phase and the magnitude are calculated in the I/Q-demodulation mode. In this mode, two signals are generated which are proportional to the real and imaginary part of the impedance and must be sampled individually.

Tab. 1: Calibration network consisting of four resistances used for the AFE4300.

R_{00}	R_{01}	R_{10}	R_{11}
14,9 Ω	46,97 Ω	679 Ω	995 Ω

We use the full-wave rectifier, however, in a different mode where only the magnitude of the impedance signal is determined. Therefore, the voltage drop at the impedance is calculated by injecting a sinusoidal current using

$$u(t) = A|Z|\sin(\omega_0 t + \theta). \tag{1}$$

Here, Z is the magnitude and θ is the phase of the impedance at given frequency ω_0. The resulting DC value, which is proportional to the magnitude, is rectified by the AFE4300 as described in

$$DC = \frac{2}{T}\int_{\frac{T}{2}} A|Z|\sin(\omega_0 t + \theta)\,\mathrm{d}t = \frac{2A|Z|}{\pi} = K|Z|. \tag{2}$$

The factor K is then determined with the calibration resistances. The full-wave rectification is much faster and the

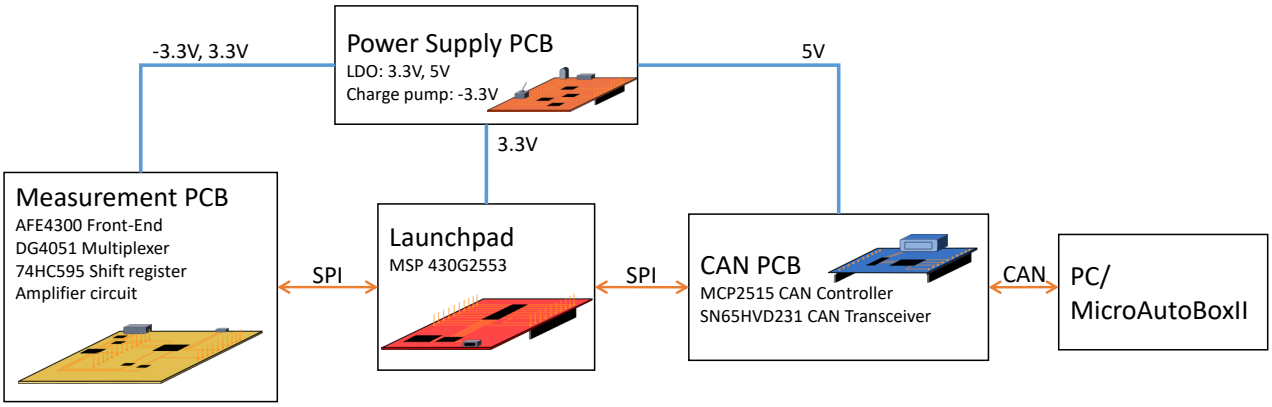

Fig. 2: Schematic overview of the modular layout of the impedance measurement unit.

calibration needs to be performed at only one measurement frequency. Please refer to the data sheet [13] for a full description of features of the AFE4300 and the implementation of the serial peripheral interface communication.

A resistance of 1 kΩ to limit the current amplitude for cardiac current injection and a capacitance of 1 μF for the suppression of DC voltages were inserted into the injecting path. This leads to an effective injected current amplitude of about 254 μA.

The *in vitro* models and the measurement system developed are going to be integrated into the heart volume test bench presented in an earlier work [14]. Therefore, a CAN bus was implemented to guarantee corresponding communication standards. The CAN-PCB includes a CAN controller and a transceiver that communicate via serial peripheral interface with the microcontroller. All signals on the CAN bus are collected by the MicroAutoBox II (dSPACE GmbH, Paderborn, Germany), which runs in real-time. The MicroAutoBox II is used as an overall system to adapt all parameters in real-time and record all quantities measured. The user interface developed displays the impedances of all segments of the catheter measured individually. In addition, the measurement frequency, the sampling rate of the AFE4300, and the selection of the calibration resistances are visualized and can be changed during the measurement.

In silico model

A FE model of the left ventricle was designed in CST STUDIO SUITE 2018 (Providence, Rhode Island, USA) to validate and further analyze the left ventricle phantoms presented in section *Ventricle phantom*. An overview of the model is shown in Figure 3. CST is a tool for the analysis of electromagnetic fields. CST EM Studio, which is particularly suitable for low frequency and quasi-static applications, was applied. All simulations were performed using a tetrahedral mesh representation of the model and solved with the "Low Frequency Domain Solver." Mesh quality and computational costs were improved by applying adaptive mesh refinement. Simplistic geometric shapes can be inserted and combined in CST via Boolean operations. The import of surface data (.stl files) is also possible but has limitations for complex geometries.

The material properties of the ventricle were set based on the measurements from [10]. The conductivity of pure silicone was chosen to be $\sigma_{\text{Ventricle}} = \sigma_{\text{Silicone}} = 10^{-10}\,\frac{\text{S}}{\text{m}}$ to simulate the insulating ventricle, whereas silicone enriched with carbon was set to $\sigma_{\text{Ventricle}} = \sigma_{\text{Carbon}} = 0.306\,\frac{\text{S}}{\text{m}}$. The CAD data used for the development of the *in vitro* model was migrated to CST and the ventricle was modeled inside a water tank. In addition, the blood cavity was designed to have a conductivity of $\sigma_{\text{Saline}} = 0.658\,\frac{\text{S}}{\text{m}}$, which is similar to the measured conductivity of the saline solution (see section *Ventricle phantom*). The model of the water tank including the ventricle with adaptable material properties is shown on the left side in Figure 3. A simple cylindrical structure was used to model the tank. The PVC hose is modeled as a hollow cylinder with material properties of PVC. The electrophysiology catheter is realized by placing cylindrical segments on top of each other. The electrodes are modeled as perfect electric conducting material in contrast to the segments between electrodes, which are modeled as PVC. The catheter and its central location in the left ventricle can be seen in Figure 3 on the right side. The positioning of the catheter is variable, as indicated by the arrows. We use a tetrahedral mesh type, which allows for accurate modeling of complex structures. The model presented consists of 312,128 tetrahedrons with an average mesh quality of 0.755; a quality of 1 being the optimum and a value of 0 being the worst (Fig. 3, middle).

An alternating voltage of 0.1 V (peak-to-peak) with a frequency of 64 kHz, which is inside the beta dispersion range, was set at the outer electrodes (1 and 10) for the simulation,

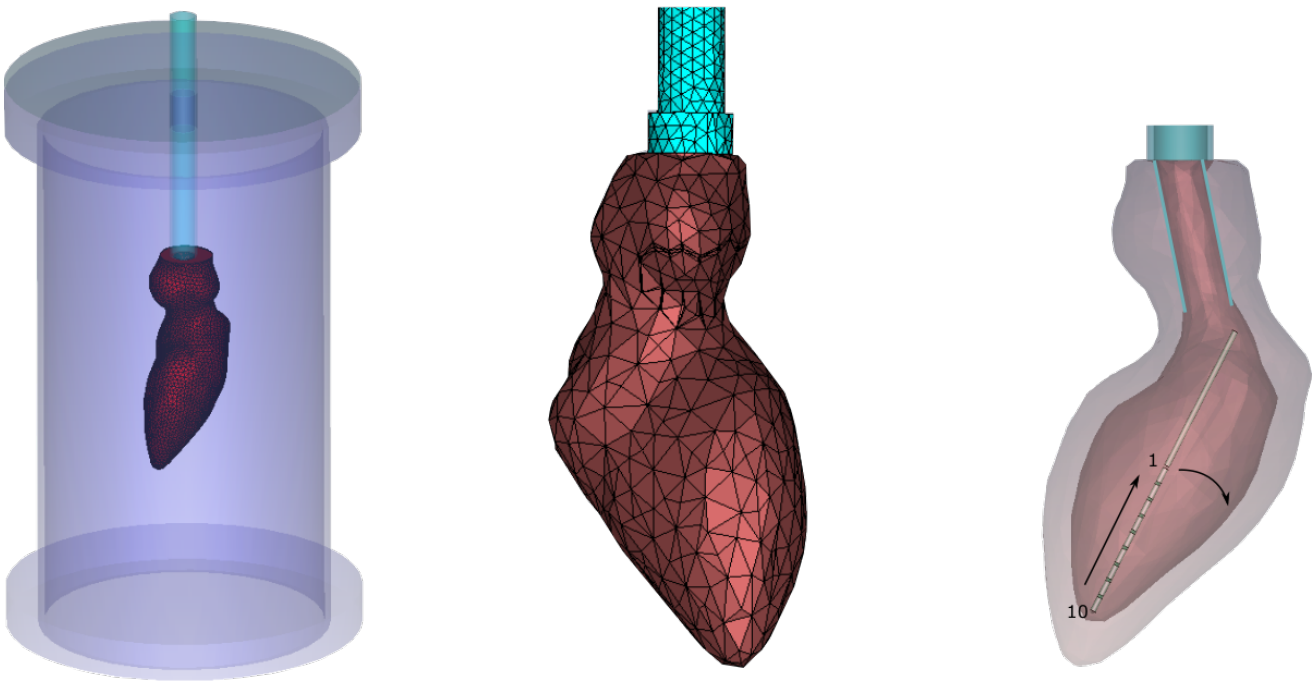

Fig. 3: Left: *In silico* FE model similar to the *in vitro* model from CAD files; middle: Mesh view of the FE model; right: Close-up of the ventricle's longitudinal cross-section with the ten-electrode catheter.

as it is not possible to inject current for tetrahedral meshes in CST. This mesh type is necessary for modeling fine structures, resulting in the application of a fixed potential, which corresponds to the fixed current injected in the measurements. The resulting current can be obtained by the integration of the current density on a predefined analytical face. The face was chosen to be in the cutting plane parallel to the injecting electrodes. The current calculated is between 220 μA and 290 μA, close to the current applied from the *in vitro* measurement setup. The impedance can be calculated from this according to Ohm's law. The analysis and all further calculations were made in MATLAB (MathWorks, Natick, Massachusetts, USA).

Ethical approval

The conducted research is not related to either human or animals use.

Results and Discussion

Impedance measurement system

The validation of the impedance measurement system presented was carried out by comparing its results to metal film resistors with an accuracy of $\pm 1\%$. The conversion rate of the AFE4300 was set to 4 Hz and the measurement frequency for the injected current was set to 64 kHz. Two networks of seven serial connected resistances net1 (seven resistances of 12 Ω) and net2 (seven resistances of 22 Ω) were connected to the measurement system, so that each of the seven channels was tested. One measurement of all channels in less than 250 ms reached an accuracy of 99.34 % for each channel tested with both resistance networks (net1 and net2).

In addition, we performed a sensitivity analysis of the measurement system at the measurement frequency of 64 kHz to investigate the influence of varying resistance values of one channel on the others. The analysis identifies the limitations of our system and allows the correct interpretation of measurement results. For this, one resistor of net2 is substituted with a different resistor (12.1 Ω, 33.3 Ω, 46.8 Ω or 98.4 Ω) and the conversion rate was varied between 4 Hz to 98 Hz. As a result, the overall error increases up to 10 %. This error was observed as an increase in impedance for all channels, at the highest possible conversion rate of 95 Hz and the substitution of a resistance of 98.4 Ω. This may be due to a transient phenomenon in the AFE4300, where the stationary state seems to be reached faster when similar resistances are monitored.

As we do not expect resistances with large ohmic differences between the catheter segments, it is possible for future applications to measure the cardiac cycle synchronously with high conversion rates. Since we only consider static measurements in this study, we suggest that all measurements presented have an accuracy in the range of 99.34 %.

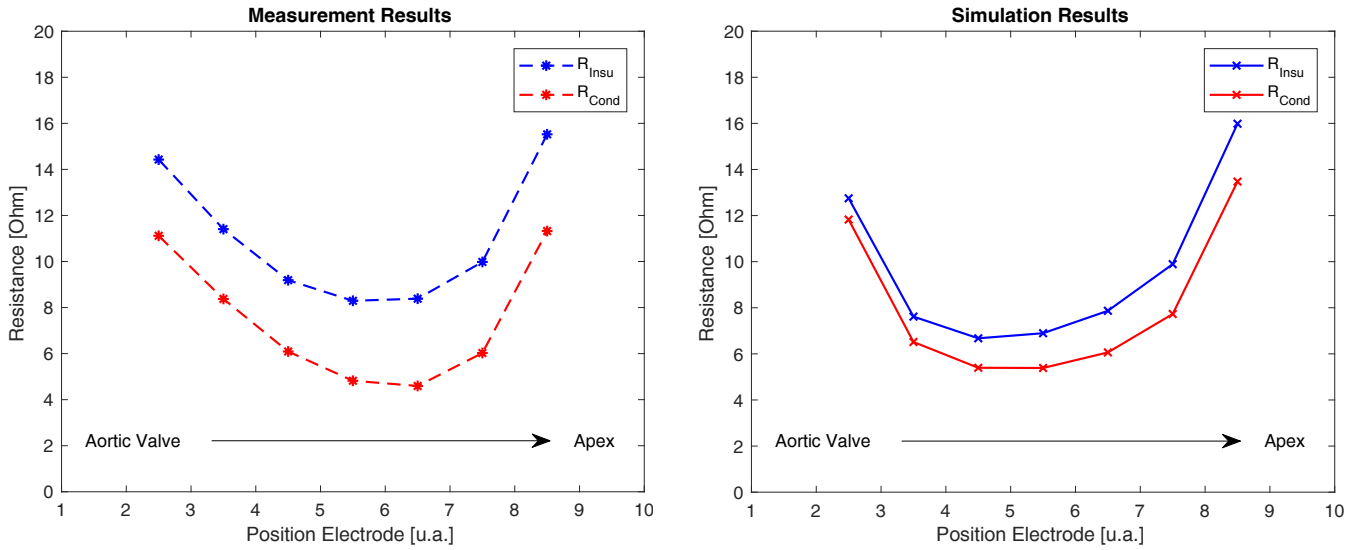

Fig. 4: Left: Measured impedances in the conductive (red) and insulating silicone ventricle (blue) impedance; right: Simulated impedances in the conductive (red) and insulating ventricle (blue).

In vitro model

The measured resistances of both ventricle phantoms are illustrated for each electrode segment in Figure 4 on the left side. The insulating ventricle is shown in blue and the conductive ventricle in red. We observed that resistances close to the apex are larger than those measured in the middle of the phantom. This confirms measurement results expected, as the volume of the blood cavity, the most conductive material, is larger in the middle than in the apex region. The minimum of the resistance measured is reached in the segment between electrodes 6 and 7. The measurements from the conductive ventricle phantom differ from the insulating ventricle measurements at an average of $-3.55\,\Omega \pm 0.198\,\Omega$. This offset is proportional to the increase in the cross-sectional area, directly referring to the thickness of the muscle wall of 8 mm - 10 mm. In the case of the insulating material, the current remains in the blood chamber, while in conductive material, parts of the injecting current flows into the ventricle myocardium. Therefore, the cross-sectional area through which all the injected current flows is smaller, leading to an overall increase in resistance in the case of the insulating phantom. The resistances measured in both ventricles show the same shape across the different segments, thus, we can assume that the catheter is similarly placed in both ventricles and that the geometry of both cast phantoms correlates well.

In silico model

A two-dimensional map of the relative current density of the simulations with insulating and conductive material is depicted in Figure 5: the current pathways of a ventricle with insulating properties are shown in the left side and the current pathways of the ventricle with conductive properties are shown on the right side. It is clearly noticeable that in the case of insulating material, the current remains in the blood chamber (Fig. 5, left), while in the case of conductive material, a significant part of the current flows into the ventricle myocardium (Fig. 5, right). All materials have been defined as discussed and the catheter was placed in a position in the middle of the ventricle.

The estimated resistances for all segments between adjacent electrodes are presented in Figure 4 on the right side. The insulating ventricle is illustrated in blue and the conductive ventricle in red. It is noticeable that higher resistances appear in the region close to the apex, whereas the lowest resistances can be observed at the segments in the middle of the catheter $(4-5)$. As discussed, this may be due to the lower volume of blood in the apex region. Comparing the insulating and the conductive ventricle, conductive muscle walls reduce impedance. On average, the difference of the resistance between both settings is $-1.612\,\Omega \pm 0.334\,\Omega$. Both curves converge at the segment close to the aortic valve $(2-3)$. As these electrodes are close to the blood filled aorta, the muscle walls show a reduced impact on the current distribution at the catheter.

Comparison of the in vitro and in silico model

A similar catheter position in both scenarios had to be found for the comparison of measurements obtained at the *in vitro* models and the simulation results from the *in silico* model. The catheter in the FE model can be shifted and rotated as indicated by the arrows on the right side in Figure 3. One of the difficulties in this study was the placement of the electrode catheter in the silicone phantoms, since the phantoms are not

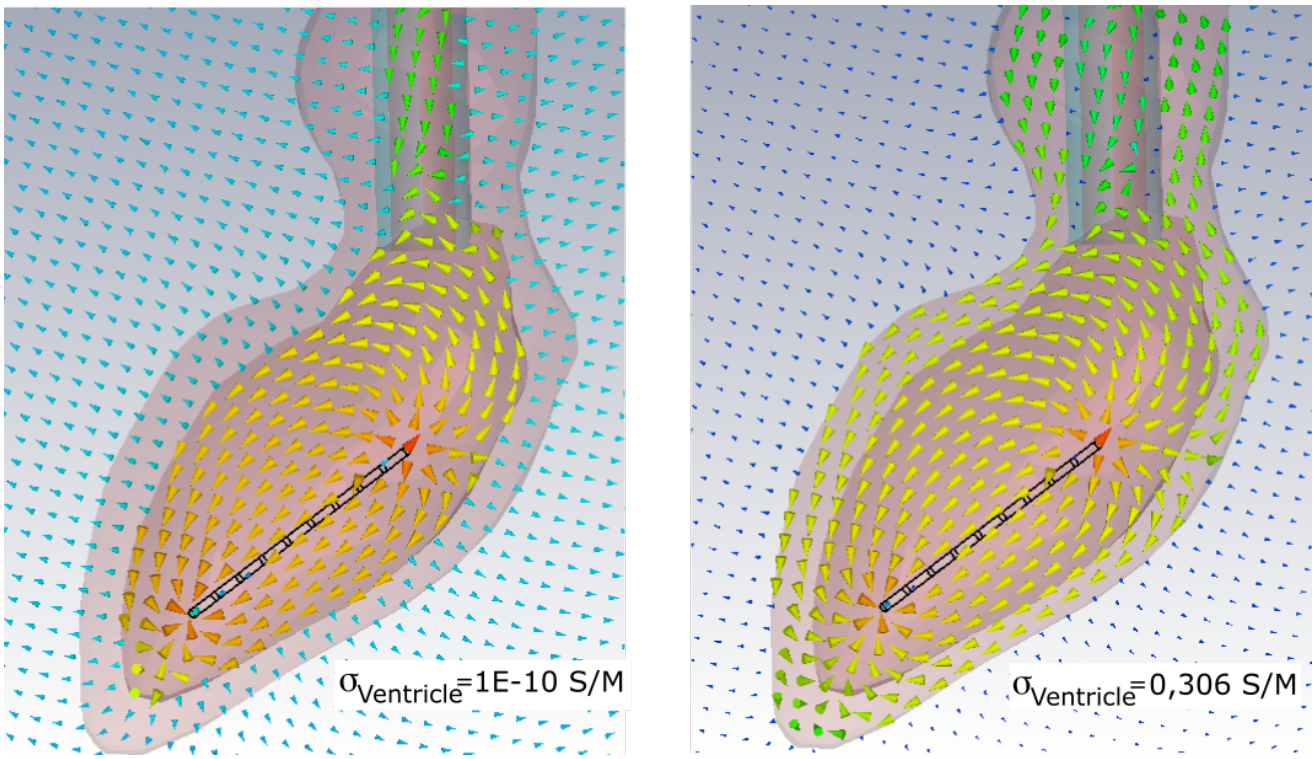

Fig. 5: Close-up of the current paths in the ventricle with insulating properties (left) and conductive properties (right).

transparent. To solve this problem, we set a fixed insertion distance of 9 cm from electrode 1 to the beginning of the PVC hose. With this setup the assumed catheter position is central in the ventricle without touching the phantom walls. In the FEM simulation, a distance of 9 cm from electrode 1 to the end of the ventricle, where only the PVC hose remains, was set. The results shown in Figure 5 and 4 are taken with this catheter location.

Looking at the results from Figure 4 and comparing measurements (left) and simulations (right), it can be observed that the shapes of the curves are quantitatively similar. The assumption from section *Impedance measurement system* that resistances measured for different segments are within a narrow ohmic range ($\pm 4\,\Omega$) is validated with the simulations, suggesting that the measurement system presented allows for highly accurate impedance monitoring. Comparing measurement and simulation results, it can be noticed that a shift of resistance minima appears from position $4-5$ in the simulation to $6-7$ in the *in vitro* models. This may be due to the fact that the real catheter is flexible and, therefore, the determination of its position is not very accurate.

Additionally, the difference of insulating to conductive material is higher in the measurements than in the simulations. A possible explanation is the difficult placement of the core inside the casting molds that may lead to a shift of wall thickness in the *in vitro* model. We suggest only using polyvinylalcohol cores for future phantom casting. Nevertheless, the resistance measurements in the area of the apex are reproduced in the simulation, concluding that this area was manufactured as planned. The simulation and measurement results differ the most closest to the connecting PVC hose. Furthermore, the difference between the conductive and the insulating ventricle is more significant in the measurements compared to the simulation. Our assumption is that the shape of the ventricle phantoms in the aortic valve area differs from the CAD model, and therefore, from the model in CST Studio. Silicone was used to glue the phantom to the PVC hose while ensuring waterproofness, which resulted in more material. Small differences in the conductivity and wall thickness of the modeled myocardium can lead to differences in absolute values observed.

Furthermore, there are some limitations of the presented study. The background material of the models was kept at a fixed conductivity of water. However, the conductivity of the surrounding tissue changes for instance by respiration (inflated: $0.104\,\frac{\mathrm{S}}{\mathrm{m}}$; deflated: $0.265\,\frac{\mathrm{S}}{\mathrm{m}}$@64kHz). This phenomenon must be taken into account for dynamic operation. In addition, the deformation of the lung has an effect on the anatomy of the heart. Therefore, the development of differently shaped hearts would be advantageous to cover a wide range of anatomic differences. Furthermore, changes in conductivity due to changes in wall thickness, as they occur in the contracting heart, should also be investigated for the developed models.

Conclusion

We developed an *in vitro* and *in silico* model of the human left ventricle. The *in vitro* model consists of two ventricle phantoms made from silicone, where one is enriched with carbon to gain a conductivity similar to heart tissue properties. A measurement system using a ten-electrode electrophysiology catheter to measure the impedance inside the phantoms was presented. A FEM simulation of the same setup was performed for *in silico* testing and compared to the results from the *in vitro* tests.

In summary, the simulation results fit well to the impedances measured inside the ventricle phantoms. We are, thus, confident that our *in vitro* and *in silico* model can be used to further investigate impedance measurements in VAD therapy. Therefore, the VAD will be integrated into the *in vitro* model inside a cardiac volume test bench [14], which simulates the remaining heart activity. Additionally, we believe to gain knowledge about potential electrode placements, to further improve the calculation of left ventricular volume for the given VAD geometry using the *in silico* model.

In addition, simulations and measurements have already been carried out to model the capacitive behavior of heart muscle tissue [15]. In future research, we will modify the ventricles and integrate bariumtitanate into silicone to achieve additional permittivity properties. Overall, the configuration presented helps to investigate cardiac impedance measurements while avoiding animal testing and, simultaneously, to continue research that improves the quality of life of patients treated with VADs.

Acknowledgment

This work has been funded by the Federal Ministry of Education and Research (BMBF, Germany) and is part of the project inHeart (grant number 13GW0118C).

Conflict of interest

Authors state no conflict of interest.

References

1. Roth GA, Johnson C, Abajobir A, Abd-Allah F, Abera SF, Abyu G, et al. Global, regional, and national burden of cardiovascular diseases for 10 causes, 1990 to 2015. Journal of the American College of Cardiology. 2017;p. 23715. http://dx.doi.org/10.1016/j.jacc.2017.04.052.

2. Chong MA, Wang Y, Berbenetz NM, McConachie I. Does goal-directed haemodynamic and fluid therapy improve peri-operative outcomes?: a systematic review and meta-analysis. European Journal of Anaesthesiology (EJA). 2018;35(7):469–483. http://dx.doi.org/10.1097/EJA.0000000000000778.

3. Stephens RS, Whitman GJR. Postoperative critical care of the adult cardiac surgical patient. Part I: routine postoperative care. Critical Care Medicine. 2015;43(7):1477–1497. http://dx.doi.org/10.1097/CCM.0000000000001059.

4. Bullister E, Reich SA, d'Entremont P, Silverman N, Sluetz J. A blood pressure sensor for long-term implantation. Artificial Organs. 2001;25(5):376–379. http://dx.doi.org/10.1046/j.1525-1594.2001.025005376.x.

5. Baan J, Van Der Velde ET, De Bruin HG, Smeenk GJ, Koops J, Van Dijk AD, et al. Continuous measurement of left ventricular volume in animals and humans by conductance catheter. Circulation. 1984;70(5):812–823. http://dx.doi.org/10.1161/01.CIR.70.5.812.

6. Wei C, Valvano JW, Feldman MD, Pearce JA. Nonlinear conductance-volume relationship for murine conductance catheter measurement system. IEEE Transactions on Biomedical Engineering. 2005;52(10):1654–1661. http://dx.doi.org/10.1109/TBME.2005.856029.

7. Schaefer M, Gross W, Ackemann J, Gebhard MM. The complex dielectric spectrum of heart tissue during ischemia. Bioelectrochemistry. 2002;58(2):171–180. http://dx.doi.org/10.1016/S1567-5394(02)00152-4.

8. Ghista DN, Vayo WH, Sandler H. Elastic modulus of the human intact left ventricledetermination and physiological interpretation. Medical and Biological Engineering. 1975;13(2):151–161. http://dx.doi.org/10.1007/BF02477722.

9. Gent AN. On the relation between indentation hardness and Young's modulus. Rubber Chemistry and Technology. 1958;31(4):896–906. http://dx.doi.org/10.5254/1.3542351.

10. Korn L, Lyra S, Rüschen D, Pugovkin A, Telyshev D, Leonhardt S, et al. Heart phantom with electrical properties of heart muscle tissue. Current Directions in Biomedical Engineering. 2018;4(1):97–100. http://dx.doi.org/10.1515/cdbme-2018-0025.

11. Emboi3D; 2017. Available from: https://www.embodi3d.com/files/file/59-heart-\ and-pulmonary-artery-tree-from-ct-angiogram/?_fromLogin=1.

12. Lang RM, Bierig M, Devereux RB, Flachskampf FA, Foster E, Pellikka PA, et al. Recommendations for chamber quantification. European Journal of Echocardiography. 2006;7(2):79–108. http://dx.doi.org/10.1016/j.euje.2005.12.014.

13. AFE4300 Datasheet;. 01.03.2018.

14. Korn L, Rumpf M. Testbench to model cardiac volume changes. POSTER 2019. 2019.

15. Korn L, Lyra S, Leonhardt S, Walter M. Analysis of silicone additives to model the dielectric properties of heart tissue. 17th International Conference on Electrical Bioimpedance ICEBI 2019. 2019; http://dx.doi.org/10.1007/978-981-13-3498-6_10.